# Dynamical spin-density waves in a spin-orbit-coupled Bose-Einstein condensate

Yan Li,[1,2] Chunlei Qu,[2] Yongsheng Zhang,[3,4,2] and Chuanwei Zhang[2,*]
[1]*Department of Physics, East China Normal University, Shanghai 200241, China*
[2]*Department of Physics, The University of Texas at Dallas, Richardson, Texas 75080, USA*
[3]*Laboratory of Quantum Information, University of Science and Technology of China, Hefei 230026, China*
[4]*Synergetic Innovation Center of Quantum Information and Quantum Physics, University of Science and Technology of China, Hefei 230026, China*
(Received 5 March 2015; published 31 July 2015)

Synthetic spin-orbit (SO) coupling, an important ingredient for quantum simulation of many exotic condensed matter physics, has recently attracted considerable attention. The static and dynamic properties of a SO-coupled Bose-Einstein condensate (BEC) have been extensively studied in both theory and experiment. Here we numerically investigate the generation and propagation of a *dynamical* spin-density wave (SDW) in a SO-coupled BEC using a fast moving Gaussian-shaped barrier. We find that the SDW wavelength is sensitive to the barrier's velocity while varies slightly with the barrier's peak potential or width. We qualitatively explain the generation of SDW by considering a rectangular barrier in a one-dimensional system. Our results may motivate future experimental and theoretical investigations of rich dynamics in the SO-coupled BEC induced by a moving barrier.

DOI: 10.1103/PhysRevA.92.013635 PACS number(s): 67.85.De, 03.75.Kk, 67.85.Fg

## I. INTRODUCTION

Spin-orbit (SO) coupling plays an important role for the emergence of many exotic quantum phenomena in condensed matter physics [1,2]. In this context, the recent experimental realization of SO-coupled neutral atoms provides an excellent platform for the quantum simulation of condensed matter phenomena because of the high controllability and free of disorder [3–6] of cold atoms. By dressing two atomic internal states through a pair of lasers, a Bose-Einstein condensate (BEC) with equal Rashba and Dresselhaus SO coupling has been achieved [3,7–12] . The static and dynamic properties of such SO-coupled BEC [13–23] have also been investigated. Notable experimental progress in SO-coupled BECs includes the observation of spin Hall effects [24] and Dicke-type phase transition [10], the study of collective excitations such as the dipole oscillation [8] and roton modes [25,26], as well as the dynamical instabilities [27] in optical lattices, etc. Recently, the generation of another type of SO coupling, the spin and orbital-angular-momentum coupling, was also proposed [28–30].

Moving potential barriers have been used in the past for the study of the superfluidity of ultracold atomic gases. For instance, by stirring a small impenetrable barrier back and forth in a condensate, the evidence of the critical velocity for a superfluid was observed [31]. When a wider and penetrable barrier was swept through a condensate at an intermediate velocity, the condensate is filled with dark solitons [32].

In this paper, we study the moving barrier induced dynamics in a SO-coupled BEC. We find that a fast moving penetrable barrier may generate a dynamical spin-density wave (SDW) in the wake of the barrier. Static SDW, which was proposed in solid state physics by Overhauser [33,34], has been widely studied in many different solid state materials such as chromium [35,36]. Our generated SDW in a SO-coupled BEC is induced by the moving barrier and vanishes when the SO coupling is turned off. The spatial periodic modulation of the spin density is not static, i.e., the local spin polarization oscillates in time periodically, and could last for a very long time.

The paper is organized as follows. Section II describes the model of the SO-coupled BEC. In Sec. III, we study the dynamics induced by a suddenly turned-on stationary barrier or a slowly moving barrier. Section IV includes the main results of the paper. We generate a dynamical SDW with a fast moving barrier, study its propagation, parameter dependence, and finally explain its mechanism using a simple one-dimensional (1D) system. Section V is the discussion.

## II. THEORETICAL MODEL

The SO-coupled BEC is realized by shining two counterpropagating laser beams on cold atoms [3]. Two atomic internal states can be regarded as pseudospins $|\uparrow\rangle = |F = 1, m_F = 0\rangle$ and $|\downarrow\rangle = |F = 1, m_F = -1\rangle$ of $^{87}$Rb atoms. To stimulate the two-photon Raman transitions, the two lasers are chosen to have a frequency difference comparable with the Zeeman splitting $\hbar\omega_Z$ between two spin states. The experimental configuration and level diagram are shown in Fig. 1. In our simulations, we consider a realistic elongated BEC with $N = 10^4$ atoms in a harmonic trap with trapping frequencies $\omega_{x,y,z} = 2\pi \times \{20, 120, 500\}$ Hz. The strong confinement along the $z$ and $y$ directions reduces the dimension to quasi-1D. We use $E_r = \hbar^2 k_L^2/2m$ as the energy unit, where $k_L$ is the recoil momentum along the $x$ direction (i.e., the SO-coupling direction).

A barrier, which can be created by the dipole potential of another laser beam [31,32], is suddenly switched on in the BEC or is swept from the left to the right side with a velocity of $v$ ranging from 1 to 80 $\mu$m/ms. The barrier peak potential is 5–25 $E_r$, which is much larger than the chemical potential of the system. The width of the barrier is at the order of $\mu$m. The external potential barrier sweeping through the BEC is

*chuanwei.zhang@utdallas.edu

 

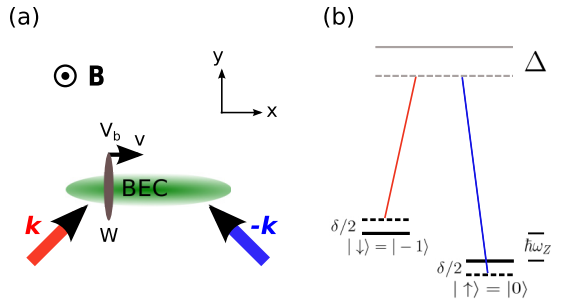


FIG. 1. (Color online) (a) Experimental setup for the observation of barrier induced dynamics in a SO-coupled BEC. The realistic barrier, created by another external laser beam, is characterized by the width $W$ (along $x$ direction), barrier peak potential $V_b$, and barrier velocity $v$. (b) Energy level diagram of the SO-coupled BEC. Two internal states are coupled by the two-photon Raman transition through a pair of counterpropagating Raman beams.

modeled as a Gaussian potential of the form,

$$V(\mathbf{r},t) = V_b e^{-\frac{(x-x_0-vt)^2}{2w_x^2} - \frac{y^2}{2w_y^2} - \frac{z^2}{2w_z^2}}, \tag{1}$$

where $w_x = W$ is the Gaussian barrier width along the SO-coupling direction. $w_{y/z}$ are much larger than the BEC widths in these two directions. $x_0$ and $v$ are the initial position and velocity of the barrier potential; $V_b$ is the peak potential of the barrier.

The dynamics of the SO-coupled BEC are governed by the Gross-Pitaevskii (GP) equation:

$$i\hbar\frac{\partial}{\partial t}\psi = [H_{\rm SO} + V_{\rm trap} + V(\mathbf{r},t) + H_I]\psi, \tag{2}$$

where the single-particle Hamiltonian with SO coupling is given by

$$H_{\rm SO} = \frac{\hbar^2}{2m}(\mathbf{k} + k_L\sigma_z\hat{e}_x)^2 + \frac{\delta}{2}\sigma_z + \frac{\Omega}{2}\sigma_x, \tag{3}$$

where $\sigma_i$ $(i = x,y,z)$ are the Pauli matrices, $\delta$ is the detuning of the Raman transition, and $\Omega$ is the Raman coupling strength. The trapping potential is of the form $V_{\rm trap} = m\omega_x^2x^2/2 + m\omega_y^2y^2/2 + m\omega_z^2z^2/2$. For the sake of simplicity, we consider a 2D geometry in our calculations by integrating out the $z$-dependent degree of freedom in the GP Eq. (2), which is valid because the strong confinement along $z$ direction restricts the BEC to the ground state of the harmonic trap along the $z$ direction, yielding

$$\psi_{3D}(\mathbf{r},t) = \psi_{2D}(x,y,t)\left(\frac{m\omega_z}{\pi\hbar}\right)^{1/4} e^{-\frac{m\omega_z}{2\hbar}z^2}. \tag{4}$$

The interaction between atoms is determined by the mean-field Hamiltonian,

$$H_I = \begin{pmatrix} g_{\uparrow\uparrow}|\psi_\uparrow|^2 + g_{\uparrow\downarrow}|\psi_\downarrow|^2 & 0 \\ 0 & g_{\downarrow\uparrow}|\psi_\uparrow|^2 + g_{\downarrow\downarrow}|\psi_\downarrow|^2 \end{pmatrix}, \tag{5}$$

where the reduced nonlinear coefficients for the 2D system are $g_{\uparrow\uparrow} = \frac{2\sqrt{2\pi}\hbar^2Nc_0}{ma_z}$, $g_{\uparrow\downarrow} = g_{\downarrow\uparrow} = g_{\downarrow\downarrow} = \frac{2\sqrt{2\pi}\hbar^2N(c_0+c_2)}{ma_z}$. The harmonic oscillator characteristic length is $a_z = \sqrt{\hbar/m\omega_z}$ and the $s$-wave scattering lengths are given by $c_0 = 100.86a_0$, $c_2 = -0.46a_0$ ($a_0$ is the Bohr radius).

In most cases the many-body interaction is weak, therefore many interesting physics can be well understood from the single-particle band structure, which is either a double well type (for $\Omega < 4E_r$) or a single well type (for $\Omega > 4E_r$) for $\delta = 0$. For $\Omega < 0.2E_r$, BEC stays in both wells and the two dressed states interfere to form a stripe pattern; for $0.2E_r < \Omega < 4E_r$, BEC chooses either of the two wells as the true ground state, which is usually called plane wave phase or magnetized phase with a finite spin polarization $|\langle\sigma_z\rangle| = \sqrt{1-(\Omega/4E_r)^2}$; for $\Omega > 4E_r$, BEC condenses at $k_x = 0$ and the spin polarization is zero $|\langle\sigma_z\rangle| = 0$. In our calculations, we focus on the latter case and take $\Omega = 6E_r$, $\delta = 0E_r$, where the generated SDW could be identified easily.

One of the effects of the SO coupling is to change the sound of speed of the condensate. For a regular BEC, the speed of sound is given by $v_s = \sqrt{U\rho/m}$, where $U = 4\pi\hbar^2Nc_0/m$ is the nonlinear coefficient and $\rho$ is the condensate density. When the BEC is dressed by the Raman lasers, the speed of sound is modified by changing the atomic mass to effective mass $m_{\rm eff}$ since the band structure of the system is modified, i.e., $v_s = \sqrt{U\rho/m_{\rm eff}}$. For experimentally relevant parameters, the speed of sound is to the order of 1 $\mu$m/ms. The speed of sound and the collective excitation spectrum has been measured in recent SO coupling experiments [25,26]. In order to generate SDW, the velocity of the moving barrier should be much larger than the speed of sound.

## III. EFFECT OF A SUDDENLY TURN-ON STATIONARY BARRIER AND A SLOWLY MOVING BARRIER

Before discussing the generation of SDW in the SO-coupled BEC through a fast moving barrier, we consider two different limits: One is that a stationary barrier is suddenly switched on in the middle of the condensate; the other one is that a slowly moving barrier is swept through the BEC from the left side to the right side. Previously, suddenly switching on a barrier potential in the middle of the superfluid is usually used to measure the speed of sound for BECs or Fermi gases [37,38]. In our calculations, the barrier potential is strong and therefore induces strong perturbations to the condensate which might be observed in experiments. Without SO coupling, the barrier excites two wave fronts propagating along both directions with the same speeds for the two spins. For SO-coupled BEC, as shown in Fig. 2, the propagation of the two wave fronts propagate differently with respect to the direction of the spin. We see that only one clear wave front propagates to the left (right) side for spin-up (down) with a speed around $\sim$10 $\mu$m/ms for the current geometry and atom number. This anisotropic and spin-dependent propagation of the density perturbation is a direct consequence of the SO coupling. Note that except the propagation of the wave fronts, a series of density modulations are excited in the mean time, which are due to the suddenly switched-on barrier induced perturbations and occur for a regular BEC as well.

When the barrier is slowly swept from the left side to the right side of the BEC, it is impenetrable for the condensate

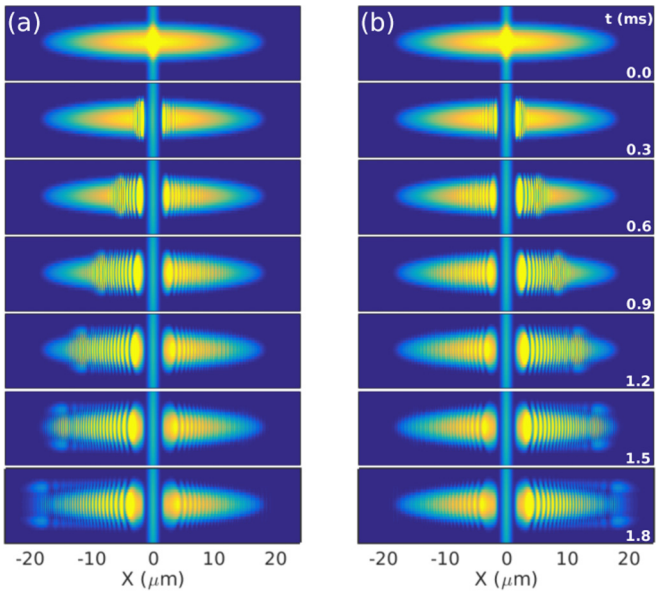


FIG. 2. (Color online) Excitation and propagation of the spin-dependent wave in a SO-coupled BEC by suddenly switching on a stationary barrier at the center of the trapped BEC at $t = 0$ ms. (a) Spin-up component; (b) spin-down component. $V_b = 10E_r$, $W = 0.5$ $\mu$m. Because of the presence of SO coupling, the propagation of sound demonstrates an anisotropic behavior, i.e., spin-up only propagates to the left side while spin-down only propagates to the right side.

because the barrier potential $V_b = 15E_r$ is much larger than the chemical potential $\sim 1$ $E_r$ of the condensate. Therefore BEC is pushed in front of the barrier with the excitations of similar density modulations for the two spins (see Fig. 3).

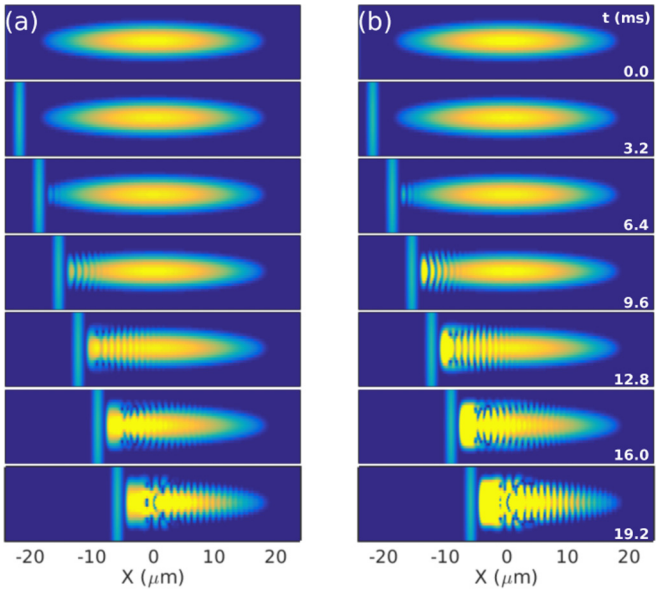


FIG. 3. (Color online) A moving barrier with low velocity $v = 1$ $\mu$m/ms pushes BEC to its right. $V_b = 15E_r$, $W = 0.5$ $\mu$m. (a) Spin-up component; (b) spin-down component.

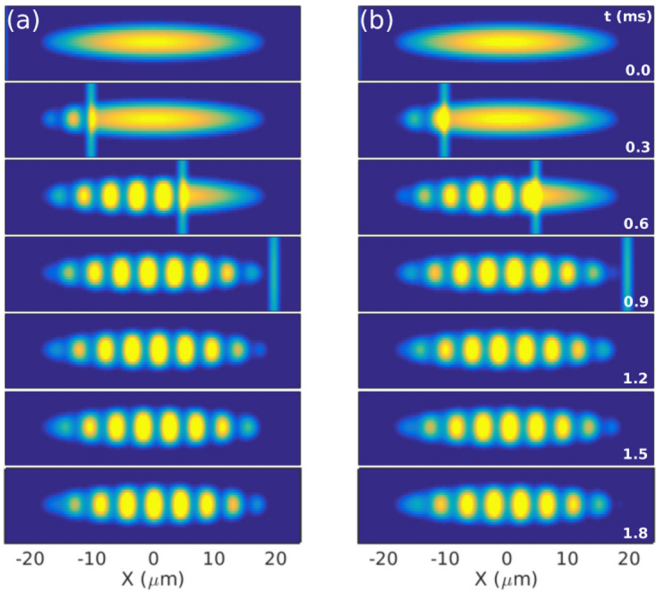


FIG. 4. (Color online) A fast moving barrier with a velocity of $v = 50$ $\mu$m/ms penetrates the BEC and generates a dynamical SDW. $V_b = 15E_r$, $W = 0.5$ $\mu$m. (a)Spin-up component; (b) spin-down component.

## IV. SDW FROM A FAST-MOVING BARRIER

In this section, we focus on a fast moving barrier with a velocity larger than the speed of sound. Because of the increasing relative velocities between the barrier and the condensate, the barrier is now a penetrable potential for the atoms. For a certain parameter regime, the barrier induces a dynamical modulation of the densities of the two spins in the wake of the barrier, while it does not lead to any observable perturbations in its front.

### A. Generation and propagation of SDW

Figure 4 shows the density distributions of two spin components when and after a moving barrier with a fast velocity is swept through the condensate. The velocity of the barrier $v = 50$ $\mu$m/ms is much larger than the speed of sound. We see that the density oscillations of the two spin components are out of phase, thus the barrier generates an SDW. The SDW could last a very long time and does not relax in the trap if all the parameters remain unchanged.

To characterize the SDW, we calculate the wavelength $\lambda$ (the distance between two peaks for one spin component) and the contrast $C_\sigma = |n^\sigma_{\max} - n^\sigma_{\min}|/|n^\sigma_{\max} + n^\sigma_{\min}|$ near the center of the BEC and plot them as a function of the barrier's peak potential $V_b$, barrier's velocity $v$, and barrier's width $W$. As shown in Fig. 5, the wavelength of the SDW is roughly a constant as a function of barrier height and width. However, the wavelength is almost proportional to the velocity of the barrier.

This is easy to understand because the SDW is not static. Each local spin polarization is fast oscillating as a function of time, as shown in Fig. 6 where we plot the local spin polarization $\langle \sigma_z \rangle (x = 0)$ in the middle of the BEC as a function of time. Before the barrier moves to $x = 0$, the density is

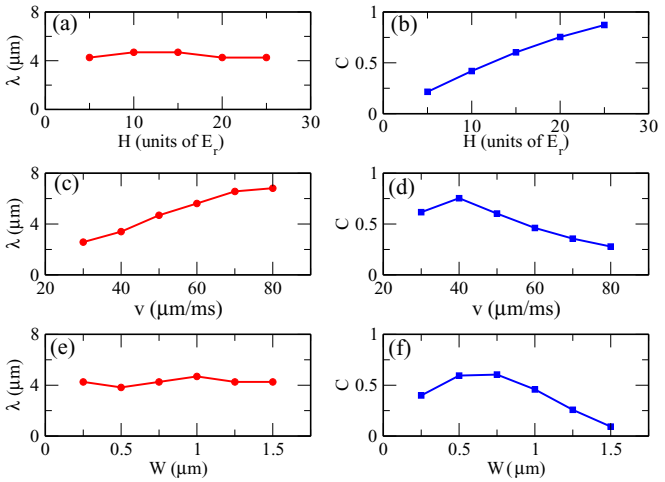


FIG. 5. (Color online) The wavelength $\lambda$ and the contrast $C$ of the SDW generated in a fast-moving barrier as a function of (a) and (b) the barrier peak potential $V_b$ for $v = 50\ \mu$m/ms, $W = 0.5\ \mu$m; (c) and (d) the barrier velocity $v$ for $V_b = 15E_r$, $w = 0.5\ \mu$m; (e) and (f) the width $W$ for $v = 50\ \mu$m/ms, $V_b = 15E_r$.

a constant. Right after the barrier is swept through $x = 0$, the densities of the two spins start *out-of-phase* oscillations, therefore there is a spin polarization oscillation. The oscillation period is roughly a constant $T$ for a certain barrier potential $V_b$. Considering that the barrier is swept through the BEC, the left and right side of the BEC is perturbed consecutively. When the barrier moves at a constant speed, the wavelength of the SDW should be proportional to the moving velocity if $T$ does not depend on the velocity significantly, i.e., $\lambda = v \times T$. Note that this relation fails to apply for much larger velocities where the spin oscillation at different local points may be generated at very short time and the above physical picture does not apply. In our numerical calculations, we verify that this oscillation curve remains the same when the interaction strength is varied in a large region, showing that the dynamical SDW is a phenomena governed by the single-particle physics. However, the phenomena changes when the interaction strength is strong enough such that the speed of sound of the condensate is comparable to the moving barrier velocity. As we have studied previously in Fig. 3, the barrier becomes impenetrable in this limit and pushes BEC to one side.

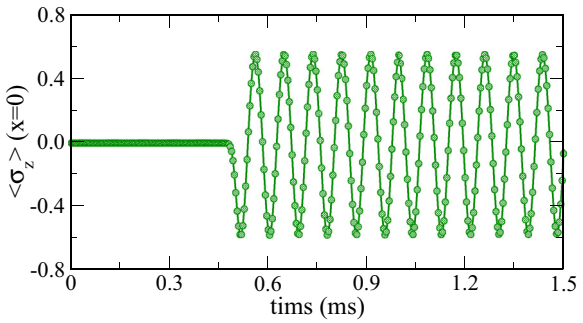


FIG. 6. (Color online) Local spin polarization $\langle\sigma_z\rangle(x = 0)$ as a function of time for Fig. 4.

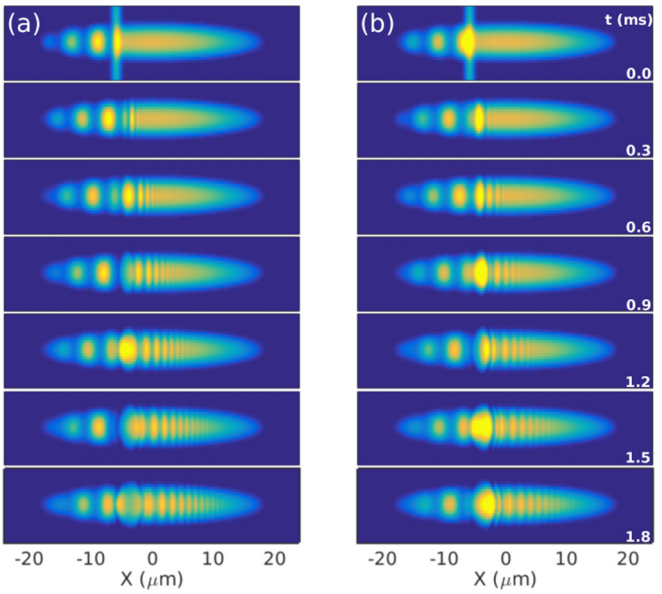


FIG. 7. (Color online) Propagation of SDW in a SO-coupled BEC. When the barrier moves to the center of the BEC, we suddenly switch off the barrier and observe the slow propagation of the SDW to the unperturbed region. All the parameters are the same as Fig. 4.

In Fig. 7, we demonstrate the slow propagation of the SDW when the barrier is suddenly turned off after it moves to the center of the BEC. Since the dynamical SDW is actually a local spin polarization oscillation instead of traveling waves, the removal of the moving barrier at the center of the BEC should stop generating SDW on its right side. However, because of the superfluidity properties of the BEC and nonlinear interactions, the unperturbed neighboring atoms will be eventually perturbed and we see that a new SDW with much smaller amplitude and velocity propagates to the right side of the BEC. The propagation of the new SDW is in the order of the speed of sound as expected.

### B. Mechanism of SDW generation

In this section, we provide a qualitative theoretical understanding of the SDW generation by considering a rectangular potential sweeping through a 1D SO-coupled BEC system. The rectangular potential can be written as

$$V(x,t) = V_b[\mathbb{H}(vt - x_0 - W) - \mathbb{H}(vt - x_0)], \tag{6}$$

where $\mathbb{H}(x)$ is Heaviside function:

$$\mathbb{H}(x) = \begin{cases} 0 & x < 0 \\ 1 & x \geqslant 0 \end{cases}. \tag{7}$$

Similar as the Gaussian barrier, here $V_b$ is the barrier potential and $W$ is the barrier width.

Figure 8 shows density distributions of the two spins at the moment when the rectangular barrier moves to a position around $X = 8\ \mu$m for different barrier widths. We see that the width of the barrier changes the generated SDW significantly. When $L$ is integer times larger than the SDW wavelength $L = n\lambda$, there are only $n$ well developed complete SDW oscillations inside the barrier and the BEC that behind the barrier seems to be unperturbed at all [Figs. 8(b)–8(d)]. When

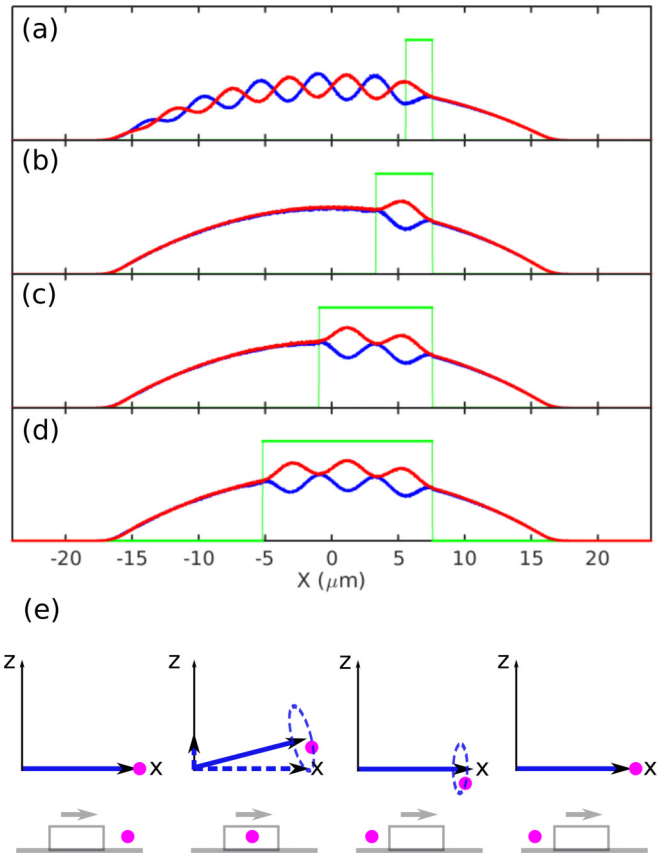


FIG. 8. (Color online) SDW generation from a rectangular barrier in 1D SO-coupled BEC system for different barrier widths (a) $W = 2\ \mu$m, (b) $W = 4.25\ \mu$m, (c) $W = 8.5\ \mu$m, (d) $W = 12.75\ \mu$m. Other parameters are $V_b = 4E_r$, $v = 50\ \mu$m/ms. (e) The dynamics of the system is equivalent to the precession of a spin under the magnetic field. Without barrier, the system is in the eigenstate of a horizontal magnetic field $B_x$. A moving barrier is equivalent to suddenly quenching on a $z$-component magnetic field $B_z$. The spin then does precession about the axis determined by the total magnetic field. When the barrier passes the point, the spin could be in any possible orientations (with SDW appears) or returns to the eigenstate of $B_x$ (no SDW appears). Other parameters are $\Omega = 6E_r$, $\delta = 0E_r$, $\omega_x = 20$ Hz.

$L$ and $\lambda$ are incommensurate, the SDW is generated in the wake of the barrier as shown in Fig. 8(a). The wavelength of the SDW is also proportional to the velocity as we have demonstrated in Fig. 5(c) for the Gaussian-shaped barrier, while rarely depends on the barrier width and height. All these features of the dynamics can be well understood in the following way.

The condensate is initially prepared at the ground state with $\Omega = 6E_r$ while the band structure has only one single minimum at $k_x = 0$, i.e., the quasimomentum of the SO-coupled BEC is zero. The initial wave function at some point $x$ is

$$\psi(x,t=0) = \frac{1}{\sqrt{2}}\begin{pmatrix}1\\-1\end{pmatrix}. \tag{8}$$

The effect of a moving barrier could be explained using a simple single-particle picture. In the laboratory frame, the real momentum of spin-up and spin-down components is $k_\uparrow = k_x + k_L = k_L$ and $k_\downarrow = k_x - k_L = -k_L$, respectively, because $k_x = 0$. An external barrier that moves along the SO-coupling direction has different relative velocities for the two spins and therefore induces spin-dependent dynamics. Take the traveling external potential as the frame of reference, the momentum are then $k_{\uparrow B} = -mv/\hbar + k_L$ for spin-up and $k_{\downarrow B} = -mv/\hbar - k_L$ for spin-down. In the presence of the fast-moving barrier, the velocities of the two spin components will be changed. From the conservation of the energy, we have the new velocities for the two spins: $k'_{\uparrow B} = -\sqrt{k_{\uparrow B}^2 - k_B^2}$ and $k'_{\downarrow B} = -\sqrt{k_{\downarrow B}^2 - k_B^2}$ where $k_B = \sqrt{2mV_b/\hbar^2} = 2k_L$ since $V_b = 4E_r$. Now converting to the laboratory frame, the velocity is $k'_\uparrow = k'_{\uparrow B} + mv/\hbar$ for spin-up, and $k'_\downarrow = k'_{\downarrow B} + mv/\hbar$ for spin-down. We find that for the large barrier velocity, $k'_\uparrow - k'_\downarrow \approx 2k_L$, which means the quasimomentum for this state is now $k'_x = (k'_\uparrow + k'_\downarrow)/2$ that agrees with the appearance of new momentum states in our GP simulations. Because of different group velocities of two spins in the presence of SO coupling, the moving barrier drives BEC to a new nonzero quasimomentum states which is equivalent to an effective detuning $\Delta_e$.

Now the SDW related phenomena could be modeled as a quench dynamics where the effective detuning $\Delta_e$ is suddenly added to induce a coupling between the two new bands. Consider the effective Hamiltonian for a two-level system (ignoring other irrelevant constants):

$$H_{\text{eff}} = \begin{pmatrix}\Delta_e/2 & \Omega/2\\ \Omega/2 & -\Delta_e/2\end{pmatrix}. \tag{9}$$

We denote $\Omega_e = \sqrt{\Omega^2 + \Delta_e^2}$, then the evolution of the local wave function for the point $x_0$ within the potential is given by

$$\psi(x_0,t) = \frac{1}{2\sqrt{2}(1-\frac{\Delta_e}{\Omega})}\begin{pmatrix}2 - \frac{3\Delta_e}{\Omega} + \frac{\Delta_e}{\Omega}e^{i\Omega_e t}\\ -2 + \frac{\Delta_e}{\Omega} + \frac{\Delta_e}{\Omega}e^{i\Omega_e t}\end{pmatrix}. \tag{10}$$

Ignoring the normalized factor and the small terms of the order $\Delta_e^2$, a straightforward calculation gives the spin polarization at this local point,

$$\langle\sigma_z(x_0,t)\rangle = C_1\frac{\Delta_e}{\Omega}[\cos(\Omega_e t) - 1], \tag{11}$$

where $C_1 > 0$.

It is quite clear that when the barrier moves to $x_0$ with a fast velocity, it perturbs the local condensate $n_\sigma(x_0,t)$ by coupling the two new bands and thus induces a *local* spin polarization oscillation $\langle\sigma_z(x_0,t)\rangle$. Due to the fact that the perturbation is applied from left to right, there is a relative phase between neighboring atoms. Therefore the spin polarization for a point on the left of $x_0$ is

$$\langle\sigma_z(x,t)\rangle = C_1\frac{\Delta_e}{\Omega}\left[\cos\Omega_e\left(t - \frac{x - x_0}{v}\right) - 1\right]. \tag{12}$$

We see from the above equation that the local spin polarization within the rectangular potential is always negative and the period of the oscillation is $T_{\text{in}} = 2\pi\hbar/\Omega_e$. Therefore the wavelength is $\lambda_{\text{in}} = 2\pi\hbar v/\Omega_e$.

Note that the point which has a separation of $n\lambda_{\text{in}}$ with the right edge of the rectangular barrier has a vanishing spin polarization. If the left edge of the barrier coincides with

these spin polarization vanishing points, i.e., $W = n\lambda_{\text{in}}$, then a striking effect occurs as we have seen from Figs. 8(b)–8(d): The condensate in the wake of the barrier seems to be unperturbed at all. That is because the potential has been removed for these points, where the dynamics is now governed by the original Hamiltonian with $\Delta_e = 0$. At the same time the wave function returns to its eigenstate with $\langle\sigma_z\rangle = 0$.

If $W \neq n\lambda_{\text{in}}$, then even though the governed Hamiltonian returns to the original one, the wave function is not in its eigenstate and the coupling between the old two bands continues with the new Rabi frequency. Therefore in the wake of the barrier, we have the period $T_{\text{out}} = 2\pi\hbar/\Omega > T_{\text{in}}$ and the wavelength $\lambda_{\text{out}} = vT_{\text{out}}$ which is a little larger than $\lambda_{\text{in}}$ because $\Omega_e$ is slightly larger than $\Omega$. Similar calculation shows that the spin polarization could be positive or negative in one period, in agreement with the GP simulation [Fig. 8(a)]. Furthermore, when $W = (2n+1)\lambda_{\text{in}}/2$, there is the largest spin polarization oscillation amplitude behind the barrier.

The dynamics of the system are equivalent to the precession of a spin under the magnetic field [Fig. 8(e)]. Without the barrier, the system is in the eigenstate of a horizontal magnetic field $B_x$ and thus does not precess. A moving barrier is equivalent to suddenly quenching on a $z$-component magnetic field $B_z$. The spin then precesses about the axis determined by the total magnetic field. When the barrier passes through the point, the spin could be in any possible orientations (with SDW appears) or returns to the eigenstate of $B_x$ (no SDW appears).

## V. DISCUSSION

In our calculation, we have chosen $\Omega = 6E_r$. Similar SDWs can also be generated for $\Omega < 4E_r$, where the initial state is polarized and the population oscillation amplitudes of the two spins are now different. If the barrier is even faster than the speed used in this paper, then all atoms are perturbed almost at the same time, therefore the local spin polarization oscillation may be in phase. Since the delay is always present no matter how small it is, the pattern may look complicated. For a two-component BEC without SO coupling, a fast-moving barrier does not induce any observable effects because the dynamics is governed by two uncoupled bands.

The two-photon recoil momentum and recoil energy correspond to a velocity of $v_r = \hbar k_L/m = 4.14\ \mu$m/ms and a kinetic energy of $1E_r$. According to our simulations, to generate the SDW with a fast moving barrier (velocity $v$, peak potential $V_b$), we need to focus on the following parameter regime:

$$KE_b \gg V_b \gg E_r, \tag{13}$$

where $KE_b = \frac{1}{2}mv^2$ is the corresponding kinetic energy of a particle with a relative speed of $|\pm v_r - v| \approx v$ (because $v \gg v_r$) respect to the barrier.

In summary, we present a scheme to observe the generation and propagation of an SDW in a SO-coupled BEC through a moving supersonic potential. The period of the SDW almost does not change with respect to the peak potential and width of the barrier. However, it is very sensitive to the velocity of the barrier. The essence of the SDW is due to the different group velocities of the two spin components in the presence of SO coupling. The SDW could last a long time in the trap without relaxation and therefore provides a good system to study other complicated dynamics. For instance, by lowering the Raman coupling and changing the band structure, we may observe the opposite motion of the density modulations of the two spins and their relaxation in the presence of SO coupling. Furthermore, in another parameter regime (smaller barrier potential or velocity) or with a much narrower stirring barrier, it is possible to generate solitons or vortices.

## ACKNOWLEDGMENTS

We thank Peter Engels for useful discussions. Y. Li is supported by NSFC under Grant No. 11104075, and the China Scholarship Council. C. Qu and C. Zhang are supported by ARO (Grant No. W911NF-12-1-0334) and AFOSR (Grant No. FA9550-13-1-0045). Y. Zhang is supported by NSFC (Grant No. 61275122), the National Fundamental Research Program (Grants No. 2011CB921200 and No. 2011CBA00200), K. C. Wong Education Foundation, and CAS.

[1] M. Z. Hasan and C. L. Kane, Colloquium: Topological insulators, Rev. Mod. Phys. **82**, 3045 (2010).

[2] X.-L. Qi and S.-C. Zhang, Topological insulators and superconductors, Rev. Mod. Phys. **83**, 1057 (2011).

[3] Y.-J. Lin, K. Jiménez-García, and I. B. Spielman, Spin-orbit-coupled Bose-Einstein condensates, Nature (London) **471**, 83 (2011).

[4] P. Wang, Z.-Q. Yu, Z. Fu, J. Miao, L. Huang, S. Chai, H. Zhai, and J. Zhang, Spin-orbit coupled degenerate Fermi gases, Phys. Rev. Lett. **109**, 095301 (2012).

[5] L. W. Cheuk, A. T. Sommer, Z. Hadzibabic, T. Yefsah, W. S. Bakr, and M. W. Zwierlein, Spin-injection spectroscopy of a spin-orbit coupled Fermi gas, Phys. Rev. Lett. **109**, 095302 (2012).

[6] R. A. Williams, M. C. Beeler, L. J. LeBlanc, K. Jiménez-García, and I. B. Spielman, Raman-induced interactions in a single-component Fermi gas near an $s$-wave feshbach resonance, Phys. Rev. Lett. **111**, 095301 (2013).

[7] Z. Fu, P. Wang, S. Chai, L. Huang, and J. Zhang, Bose-Einstein condensate in a light-induced vector gauge potential using 1064-nm optical-dipole-trap lasers, Phys. Rev. A **84**, 043609 (2011).

[8] J.-Y. Zhang, S.-C. Ji, Z. Chen, L. Zhang, Z.-D. Du, B. Yan, G.-S. Pan, B. Zhao, Y.-J. Deng, H. Zhai, S. Chen, and J.-W. Pan, Collective dipole oscillations of a spin-orbit coupled Bose-Einstein condensate, Phys. Rev. Lett. **109**, 115301 (2012).

[9] C. Qu, C. Hamner, M. Gong, C. Zhang, and P. Engels, Observation of Zitterbewegung in a spin-orbit-coupled Bose-Einstein condensate, Phys. Rev. A **88**, 021604(R) (2013).

[10] C. Hamner, C. Qu, Y. Zhang, J. Chang, M. Gong, C. Zhang, and P. Engels, Dicke-type phase transition in a spin-orbit-coupled Bose Einstein condensate, Nat. Commun. **5**, 4023 (2014).

[11] A. J. Olson, S.-J. Wang, R. J. Niffenegger, C.-H. Li, C. H. Greene, and Y. P. Chen, Tunable Landau-Zener transitions in a spin-orbit-coupled Bose-Einstein condensate, Phys. Rev. A **90**, 013616 (2014).

[12] K. Jimenéz-García, L. J. LeBlanc, R. A. Williams, M. C. Beeler, C. Qu, M. Gong, C. Zhang, and I. B. Spielman, Tunable Landau-Zener transitions in a spin-orbit-coupled Bose-Einstein condensate, Phys. Rev. Lett. **114**, 125301 (2015).

[13] J. Dalibard, F. Gerbier, G. Juzeliūnas, and P. Öhberg, Colloquium: Artificial gauge potentials for neutral atoms, Rev. Mod. Phys. **83**, 1523 (2011).

[14] N. Goldman, G. Juzeliūnas, P. Öhberg, and I. B. Spielman, Light-induced gauge fields for ultracold atoms, Rep. Prog. Phys. **77**, 126401 (2014).

[15] C. Wang, C. Gao, C.-M. Jian, and H. Zhai, Spin-orbit coupled Spinor Bose-Einstein condensates, Phys. Rev. Lett. **105**, 160403 (2010).

[16] C. Wu, I. Mondragon-Shem, and X.-F. Zhou, Unconventional Bose-Einstein condensations from spin-orbit coupling, Chin. Phys. Lett. **28**, 097102 (2011).

[17] T.-L. Ho and S. Zhang, Bose-Einstein condensates with spin-orbit interaction, Phys. Rev. Lett. **107**, 150403 (2011).

[18] Y. Zhang, L. Mao, and C. Zhang, Mean-field dynamics of spin-orbit coupled Bose-Einstein condensates, Phys. Rev. Lett. **108**, 035302 (2012).

[19] H. Hu, B. Ramachandhran, H. Pu, and X.-J. Liu, Spin-orbit coupled weakly interacting Bose-Einstein condensates in harmonic traps, Phys. Rev. Lett. **108**, 010402 (2012).

[20] T. Ozawa and G. Baym, Stability of ultracold atomic Bose condensates with rashba spin-orbit coupling against quantum and thermal fluctuations, Phys. Rev. Lett. **109**, 025301 (2012).

[21] Y. Li, L. P. Pitaevskii, and S. Stringari, Quantum tricriticality and phase transitions in spin-orbit coupled Bose-Einstein condensates, Phys. Rev. Lett. **108**, 225301 (2012).

[22] Y. Xu, Y. Zhang, and B. Wu, Bright solitons in spin-orbit-coupled Bose-Einstein condensates, Phys. Rev. A **87**, 013614 (2013).

[23] Y. Zhang and C. Zhang, Bose-Einstein condensates in spin-orbit coupled optical lattices: Flat bands and superfluidity, Phys. Rev. A **87**, 023611 (2013).

[24] M. C. Beeler, R. A. Williams, K. Jiménez-García, L. J. LeBlanc, A. R. Perry, and I. B. Spielman, The spin Hall effect in a quantum gas, Nature (London) **498**, 201 (2013).

[25] M. A. Khamehchi, Y. Zhang, C. Hamner, T. Busch, and P. Engels, Measurement of collective excitations in a spin-orbit-coupled Bose-Einstein condensate, Phys. Rev. A **90**, 063624 (2014).

[26] S.-C. Ji, L. Zhang, X.-T. Xu, Z. Wu, Y. Deng, S. Chen, and J.-W. Pan, Softening of Roton and Phonon modes in a Bose-Einstein condensate with spin-orbit coupling, Phys. Rev. Lett. **114**, 105301 (2015).

[27] C. Hamner, Y. Zhang, M. A. Khamehchi, M. J. Davis, and P. Engels, Spin-orbit-coupled Bose-Einstein condensates in a one-dimensional optical Lattice, Phys. Rev. Lett. **114**, 070401 (2015).

[28] K. Sun, C. Qu, and C. Zhang, Spin-orbital angular momentum coupling in Bose-Einstein condensates, Phys. Rev. A **91**, 063627 (2015).

[29] M. Demarco and H. Pu, Angular spin-orbit coupling in cold atoms, Phys. Rev. A **91**, 033630 (2015).

[30] C. Qu, K. Sun, and C. Zhang, Quantum phases of Bose-Einstein condensates with synthetic spin-orbital-angular-momentum coupling, Phys. Rev. A **91**, 053630 (2015).

[31] C. Raman *et al.*, Evidence for a critical velocity in a Bose-Einstein condensed gas, Phys. Rev. Lett. **83**, 2502 (1999).

[32] P. Engels and C. Atherton, Stationary and nonstationary fluid flow of a Bose-Einstein condensate through a penetrable barrier, Phys. Rev. Lett. **99**, 160405 (2007).

[33] A. W. Overhauser, Giant spin density waves, Phys. Rev. Lett. **4**, 462 (1960).

[34] A. W. Overhauser, Spin density waves in an electron gas, Phys. Rev. **128**, 1437 (1962).

[35] E. Fawcett, Spin-density-wave antiferromagnetism in chromium, Rev. Mod. Phys. **60**, 209 (1988).

[36] C. Lester, S. Ramos, R. S. Perry, T. P. Croft, R. I. Bewley, T. Guidi, P. Manuel, D. D. Khalyavin, E. M. Forgan, and S. M. Hayden, Field-tunable spin-density-wave phases in $Sr_3Ru_2O_7$, Nature Materials **14**, 373 (2015).

[37] M. R. Andrews, D. M. Kurn, H.-J. Miesner, D. S. Durfee, C. G. Townsend, S. Inouye, and W. Ketterle, Propagation of sound in a Bose-Einstein condensate, Phys. Rev. Lett. **79**, 553 (1997).

[38] J. Joseph, B. Clancy, L. Luo, J. Kinast, A. Turlapov, and J. E. Thomas, Measurement of sound velocity in a Fermi gas near a Feshbach resonance, Phys. Rev. Lett. **98**, 170401 (2007).